Chapter 5

Modulation and Coding

Two major goals of wireless communication systems are high capacity and high quality. Both these goals are dominated by the choice of modulation and channel coding. Traditionally, high capacity was obtained when the bandwidth of the transmitted signal was kept narrow, but with the introduction of wideband techniques like CDMA, this is not necessarily true anymore. A narrow spectrum gives preference to high coding rates and high signaling constellations, which does not necessarily give high quality on a wireless channel. In CDMA, a low coding rate is not a problem, since the signal is spread in bandwidth anyway. However, it is of utmost importance that many users can exist simultaneously in the given system bandwidth. Large signaling constellations often give rise to problems with large amplitude variations in amplifiers and high sensitivity to noise and interference, which can be avoided by using smaller constellations. These are just some examples to show the importance of modulation and coding.

In FRAMES, a lot of effort has been directed towards improving modulation and coding, and some of the results will be reported in this chapter. In Section 5.1, a new multilevel modulation method is presented that gives a good possibility of trading spectral efficiency and bit error probability. Multicode CDMA, which is proposed in UTRA/FDD to handle large data rates, is described in Section 5.2. It has the disadvantage of large amplitude variations, but here a precoding scheme is given that at least partly overcomes this problem.

Turbo coding is a relatively new channel coding technique, which has been shown to have a performance close to the theoretical limits. This technique has been evaluated in great detail for UTRA/TDD, and some of the findings are summarized in Section 5.3. Various aspects of traditional convolutional codes are studied in Sections 5.4 to 5.7. It has been found that the convolutional codes in most textbooks can be slightly improved by changing the design criterion. Some of these new codes are discussed in Section 5.4. New multimedia types of services require that the source data rate is matched to an often limited set of channel data rates, and this may be done efficiently by convolutional codes as described in Section 5.5. In order to obtain very low error probabilities with convolutional codes, the constraint length needs to be large and the decoding complexity becomes prohibitive with Viterbi decoding. Then sequential decoding is an alternative technique, which is studied for wireless channels in Section 5.6. Section 5.7 is devoted to low rate codes that can be used for combined spreading and error

correction in CDMA systems. It has been found that large capacity improvements are possible with this technique. Both convolutional codes and a special class of block codes named TCH codes are studied. Finally, in Section 5.8, different types of ARQ schemes for packet transmission are described and evaluated. Packet data transmission is believed to be the major switching technique in future telecommunication systems, and here we show that large throughput improvements are possible by adapting the code rate to the channel.

The reader is assumed to be familiar with the modulation and coding techniques that are discussed throughout this chapter. There exist many good textbooks on these topics. We recommend [1] as an excellent text in the basics of digital communications. For more details on channel coding, we recommend [2] as a general text, and [3] for the details on turbo coding. Since some parts of this chapter are specifically devoted to the CDMA system, we can also recommend [4] and Chapters 2 to 3 of this book.

5.1 MALGMSK MODULATION SCHEMES

Continuous phase modulations (CPMs) [5] combine the characteristics of being constant envelope and bandwidth efficient modulation schemes. Among CPM, Gaussian minimum shifting keying (GMSK) is an important scheme for its spectral properties, being used for the GSM and DECT systems. A drawback of GMSK is that for low values of B_bT[1] , which guarantee high spectral efficiency, a strong ISI heavily degrades the error performance. Therefore, B_bT is set to 0.5 for DECT and to 0.3 for GSM. Linearized GMSK (LGMSK) is a linear modulation scheme that uses the pulse shaping function $C_0(t)$, derived by a linear approximation of GMSK [6]. The main advantage of LGMSK with respect to conventional GMSK is the possibility to implement a quadrature receiver which successfully eliminates the ISI for any value of BbT, therefore allowing an increase of the spectral efficiency at the expense of amplitude variation [7].

A further increase of the spectral efficiency can be achieved by multiamplitude linearized gaussian minimum shifting keying (MALGMSK) which is the multilevel linear modulation derived directly from binary LGMSK. The complex envelope of the MALGMSK signal is:

$$s_{\mathrm{MALGMSK}}(t) = \sum_i A_{2i} C_0(t - 2iT) + j \sum_i A_{2i+1} C_0(t - (2i+1)T) \qquad (5.1)$$

where A_i={–3,–1,1,3} are the transmitted symbols.

As for any other multiamplitude modulation, the increased efficiency is attained at the price of an increase in the *peak-to-average ratio* (PAR), which is defined as the ratio of the peak signal power to the average signal power. The PAR is related to the backoff required for operation with nonlinear power amplifiers, in order to prevent extra spectrum spreading. For nonconstant-envelope modulation

[1] B_bT is the normalized 3-dB-down bandwidth of the premodulation Gaussian low-pass filter used.

schemes, a nonlinear power amplifier causes degradation of the performances: the signal undergoes distortions so its demodulation is less efficient and the power spectrum is widened, thus the adjacent channel interference is increased.

To evaluate the power spectral efficiency of a modulating scheme, we used the *out-of-band power* (OBP), which indicates the fraction of power outside a certain bandwidth. In the case of MALGMSK, an adequate choice of the receiver filter, which satisfies the first Nyquist criterion, allows the complete cancellation of the ISI. This receiver filter $H(f)$ is not matched to the transmitted pulse $C_0(f)$. Therefore, it is necessary to introduce a correction factor δ, which indicates the performance degradation with respect to the ideal performance of a matched filter receiver. In Table 5.1, some results are summarized for MALGMSK for different values of B_bT and for quaternary offset QAM (Q-O-QAM) with raised cosine pulse shaping.

Table 5.1

Comparison for PAR, OBP, and δ for Different Instances of MALGMSK and Q-O-QAM

	MALGMSK (BbT=0.1)	*MALGMSK (BbT=0.15)*	*MALGMSK (BbT=0.25)*	*Q-O-QAM*
PAR [dB]	5.01	4.16	3.29	5.71
OBP-10dB	0.10	0.11	0.14	0.12
OBP-20dB	0.15	0.18	0.21	0.15
δ [dB]	1.59	0.49	0.09	0

Figure 5.1 shows the OBP for MALGMSK with B_bT=0.15 and for Q-O-QAM with rolloff factor 0.35. The results are obtained considering a solid state nonlinear power amplifier as modeled in [8], to evaluate the impact of the different values of PAR on the two modulation techniques for different values of output backoff. While the performances of both modulations deteriorate when compared to the linear amplifier case, MALGMSK performs better because of a smaller value of the PAR.

MALGMSK has flexible performance with respect to the choice of the value of the parameter B_bT. In comparison with Q-O-QAM: B_bT smaller than 0.15 allows better spectral performance at the expense of an increase in terms of BER; B_bT larger than 0.15 gives better BER performance (the factor δ decreases and also the PAR) but also lower spectral efficiency. The choice of a certain value of B_bT is then the ultimate question about MALGMSK, which depends on the overall system requirements.

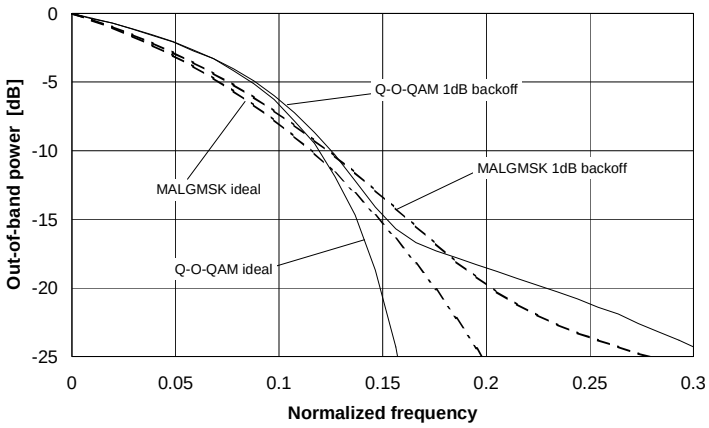

Figure 5.1 Out-of-band power for Q-O-QAM and MALGMSK (BbT=0.15). The results are plotted for the ideal case (linear amplifier) and with nonlinear, solid-state amplifier with 1dB backoff.

5.2 MULTICODE CDMA WITH PRECODING SCHEMES

In the recent WCDMA standard, variable spreading factors and multicode transmission are used to obtain multiple data rates. Variable spreading factors are used for the low and medium-high data rates, and are combined with multicode transmission for the highest data rates. The reason for this split is that for high data rates, the spreading factor in the variable spreading factor scheme will be very small and thus the performance will significantly degrade due to intersymbol interference [9]. On the other hand, using many parallel codes in the multicode scheme will result in a large envelope variation. This envelope variation results because the transmitted signal is a sum of many independently spread signals [9-11].

In a cellular phone, most of the power is consumed by the RF power amplifier, and thus the power efficiency of this amplifier is very important. A power amplifier that has high power efficiency operates near the saturation point. However, in this region, the amplitude input-output characteristics (AM-AM) of the amplifier is very nonlinear, and this nonlinearity has negative effects such as increased out-of-band radiation (spectral spreading) and decreased performance (increased bit error rate) due to bad modulation accuracy. The degree of the out-of-band radiation depends on the envelope variation of the input signal. A large variation results in a large out-of-band radiation and thus decreased spectral efficiency of the overall system. Alternatively, a large variation will decrease the power efficiency, since it forces the amplifier into the less power-efficient linear (or active) region. These arguments are the main reasons for the prevailing use of constant (or near constant) amplitude modulation schemes in cellular communica-

tion systems. It is thus also obvious that the envelope variations introduced by the multicode transmission may prohibit effective use in wireless communications, at least in the uplink, where it is of utmost importance that the handsets have a high power efficiency. It is especially true when many parallel codes are used. In this section, a precoding scheme that reduces the envelope variation is reviewed.

It was shown in [9] and [11] that the envelope variations can be drastically reduced by the introduction of a nonlinear block code called a precoder. This precoder of course depends on the set of used spreading codes, and thus the precoder must be designed specifically for that user and the spreading codes used. However, by the introduction of concatenated spreading codes, where a user-specific spreading code is element-wise multiplied by a set of Hadamard-sequences of the same length as the number of parallel codes, the precoder becomes independent of the user-specific codes [9,11]. The transmitter and receiver pair for an (n,k)-precoder are shown in Figure 5.2. Here $u(t)$ is the user-specific spreading code, $\mathbf{h}_n(t)$ the vector spreading code (a column in the Hadamard matrix of size n) of size n (the number of parallel codes), and **b** is the precoded codeword.

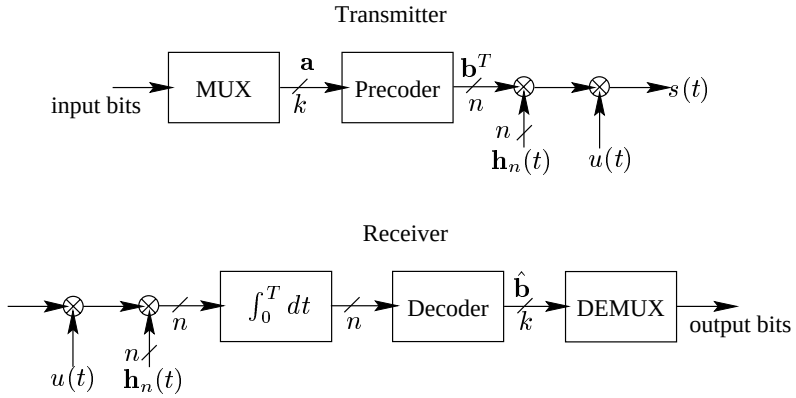

Figure 5.2 Transmitter and receiver pair for a precoded multicode DS-CDMA system using BPSK modulation.

Procedures for designing precoders are given in [11]. It is shown that the (4,3)-precoder simply is the parity-check code $\mathbf{b} = (b_1, b_2, b_3, b_4)^T=(a_1, a_2, a_3, -a_1 a_2 a_3)^T$, where $\mathbf{a} = (a_1, a_2, a_3)^T$ is the binary information word.

As a measure of the degree of envelope variations, we use the crest factor (CF), defined as the ratio between the maximum absolute value and the RMS (root mean square) value of the transmitted signal $s(t)$, respectively. Usually the CF is given in decibels. The lowest value of the crest factor is 3 dB and obtained by an unmodulated carrier. For example, a 3-code multicode scheme has a CF of 7.8 dB, while a 1-code scheme has a crest factor of 3 dB. The (4,3)-precoder introduced above has a crest factor of 3 dB, which implies that we can transmit 3 bits in parallel using four codes with the same low CF as for one-code transmission. In

addition to the decrease in envelope variation, a coding gain of about 1.5 dB compared to one-code transmission is introduced by the precoder.

Examples of other existing precoder parameters are given in Table 5.2. Given are also the CF in dB, the uncoded CF using *k*-code transmission, and the reduction in crest factor due to the precoder. As seen, the (10,4) and (16,9) precoders also results in the optimum CF of 3 dB. See [11] for more details regarding construction and performance of these precoders.

Table 5.2

Some Possible Precoder Parameters

(n,k)	CF [dB]	$CF_{uncoded}$ [dB]	$CF-CF_{uncoded}$ [dB]
(4,3)	3	7.8	4.8
(6,5)	5.6	10	4.4
(8,7)	9.5	11.5	2
(8,6)	6	10.8	4.8
(10,9)	7.4	12.6	5.2
(10,4)	3	9	6
(12,11)	7.8	13.4	5.6
(12,8)	4.3	12	7.7
(16,9)	3	12.6	9.6

5.3 EVALUATION OF TURBO CODES WITH TD-CDMA

In the following sections, the evaluation of turbo codes in the TD-CDMA concept to be used as the UTRA TDD mode is presented. First, in Section 5.3.1 the performance of turbo codes is compared to the performance of concatenated Reed-Solomon (RS) and convolutional codes by means of the results of link-level simulation. In the subsequent sections, the influence of different turbo code parameters on the system performance is considered. In detail Section 5.3.2 deals with the required minimum interleaver block size of turbo codes, Section 5.3.3 considers turbo codes with optimized interleaving, and in Section 5.3.4 the performance of turbo codes using constituent recursive-systematic-codes (RSCs) with constraint lengths 3 and 4 is compared. Finally, conclusions are drawn in Section 5.3.5.

Based on the link-level simulation programs that have been developed by the Research Group for RF Communications at the University of Kaiserslautern during the past several years, a new simulation program has been written, that is capable of performing link level simulations for TD-CDMA. This program is implemented in FORTRAN90 and was used to obtain the simulation results presented in the following sections.

5.3.1 Performance of Turbo Codes Versus Concatenated Reed-Solomon and Convolutional Codes

In the current section, the performance of concatenations of outer RS codes and inner convolutional codes and mainly the promising turbo codes is evaluated and presented. The basic principles of turbo codes are assumed to be known and not considered here, see [12, 13]. LCD services with 300 ms delay and LDD services with 50-ms delay using data rates of 64, 144, 384, 512 Kbps, and 2 Mbps are considered.

All previously enumerated service implementations have been simulated for three different mobile environments. These are characterized by the mobile radio channel models *indoor office A* (abbr. indoor*), outdoor to indoor and pedestrian A* (abbr. pedestrian) and *vehicular high antenna A* (abbr. vehicular), and were specified by the ITU, [14]. In the case of the indoor and the pedestrian channels, a mobile speed of 3 km/h and a closed loop frame-by-frame power control were used in the simulations. In the case of the vehicular channel, a mobile speed of 120 km/h was chosen and no power control was applied. The uplink simulations were carried out using two omnidirectional receiver antennas. In the downlink simulations, no antenna diversity was used. Except for the 64 Kbps service simulated with two simultaneously active users, there is no difference between the uplink and the downlink, because multiple access interference is only caused by pooled codes of one and the same user.

As an example, the performances of a turbo code and a concatenated RS and convolutional code for an LCD service with 300-ms delay and 144 Kbps data rate, evaluated for different environments, will be discussed. A turbo code with constraint length 3 and a total code rate of 0.58 is implemented, using optimum maximum-a-posteriori (MAP) symbol estimation in the decoder and a nonoptimized interleaving of the user data block. The user data block for one channel interleaving frame consists of 43,200 bits and is split into five single user data blocks of 8,640 bits which are coded and decoded separately. This means that the turbo code interleaver block size is in this case 8,640 bits. After five iterations the service implementation using the turbo code needs about 4.3 dB E_b/N_0 at the receiver input to reach the target bit error probability of 10^{-6}.

The service protected by the code concatenation is implemented with a (127,120) RS code using 8-bit symbols, and a convolutional code with constraint length 9 and mother code rate 0.5. The total code rate of the code concatenation is 0.58 and the target bit error probability of 10^{-6} is reached at 5.9 dB. In this case, the turbo code implementation of the considered service is about 1.5 dB better than the simulated code concatenation. The computational complexity of the two considered schemes is approximately the same.

For almost all simulated services and environments, the turbo code implementation of the considered service shows a gain of approximately 1 to 3 dB compared to the concatenated codes. In some cases for LDD services and the vehicular channel simulated without power control at a mobile speed of 120 km/h, the bit error curve according to the code concatenation even runs into an error floor

above the target bit error probability of 10^{-6}. The turbo code reaches the target bit error probability even with these simulation parameters.

Since the concatenation of the RS code and the convolutional code is not optimized, the performance of the code concatenation could be improved by harmonizing the codes. Nevertheless, the service implementation with turbo codes is still expected to require an E_b/N_0 at the receiver input, to reach the target bit error probability of 10^{-6}, which is significantly below that of an optimized concatenated RS and convolutional code.

5.3.2 Minimum Required Turbo Code Interleaver Block Size

In order to evaluate the influence of the interleaver block size of the turbo code interleaver on the error correction capability of the turbo code, see also [15], several simulations were carried out, and the obtained results are presented in this section. One LCD service with 300 ms delay and one LDD service with 50 ms delay were investigated, both providing a data rate of 144 Kbps and using one time slot per frame with pooling of nine CDMA codes. In the case of the LCD service, the channel interleaving frame consists of 30 frames and the total user data block size for one interleaving block is 43,200 bits. For the LDD service, the user block size of one channel interleaving frame is 7,200 bits, and the block is interleaved over five consecutive frames.

For all simulations the indoor channel at a mobile speed of 3 km/h was chosen, using frame by frame power control implemented in a closed loop fashion. No antenna diversity is applied, and since there is only one active user, the simulations are valid for the downlink as well as for the uplink. A turbo code with constraint length 3 and optimum MAP symbol estimators in the decoder is considered, and five decoding iterations are carried out. For fixed parameter settings, bit error probability curves for different sizes of the turbo code interleaver were simulated using the indoor channel at 3 km/h. In the case of the 50 ms delay service, block lengths of 200, 400, 600, 1,200, 2,400, 3,600 and 7,200 bits were considered and for the LCD service with 300 ms delay block lengths of 200, 400, 600, 1,200, 2,400, 4,800, 14,400 and 43,200 bits were evaluated. In the case of the maximum possible interleaver size of 7,200 bits for the LDD service and 43,200 bits for the LCD service, the user data block of one channel interleaving frame was coded as a whole. For smaller interleaver sizes, the channel interleaving user data block was split into smaller partitions and each partition is coded and decoded separately. The pseudorandom turbo code interleavers are not optimized and were implemented according to the scheme described in Section 5.3.3.

Both for the service with 300 ms delay and for the service with 50 ms delay, the bit error curves get steeper with increasing block length and reach the target bit error probability of 10^{-6} at decreasing E_b/N_0. For the LDD service, an E_b/N_0 of 9.5, 9 dB, approximately 8.6 and 8.2 dB is needed to achieve the target bit error rate of 10^{-6} in the case of the block lengths of 200 bits, 400 bits, 600 bits, and 1,200 bits, respectively. Using a block length of 1,200 bits instead of a block length of 200 bits we achieve a gain of 1.3 dB. Larger block lengths as 1,200 bits lead only to

little additional performance improvement. Therefore, in the case of the LDD services with 50 ms delay, a block length of 1,200 bits is sufficient, if we assume non-optimized turbo code interleavers. As will be shown in Section 5.3.3, it is possible to achieve the same performance for block lengths shorter than 1,200 bits, if the interleaver is optimized.

In case of the LCD services with 300 ms delay and the block lengths of 200 bits, 400 bits and 600 bits the target bit error probability of 10^{-6} is reached at 7.9 dB, approximately 7 dB and approximately 6.5 dB E_b/N_0, respectively. An E_b/N_0 of 5.8 and 5.2 dB is required for the block lengths of 1,200 bits and 2,400 bits, respectively. Using block lengths larger than 2,400 bits does not significantly enhance performance. For the LCD services a block length of 2,400 bits is sufficient to achieve acceptable performance. If optimized turbo interleavers are applied, even shorter block lengths can be used.

5.3.3 Optimization of Turbo Code Interleaving

In this section, the performance enhancement achievable by an optimization of the turbo code interleaver will be presented. In all simulated cases an LCD service with 300 ms delay and a data rate of 144 Kbps is considered. The simulations were carried out using the indoor channel model with a mobile speed of 3 km/h. A frame by frame closed loop power control was deployed, and only one receiver antenna is used. Since code pooling in one time slot is used to reach the envisaged data rate and only one user is active within one time slot, the presented results are valid for both the uplink and the downlink, respectively.

Three different turbo code interleaver block sizes were evaluated, namely a 600-, 1,200-, and a 4,800-bit interleaver. The nonoptimized interleavers were chosen as follows: Five different interleavers were obtained by a random generator. The interleavers were superficially tested using identical simulation parameters, and the best one was chosen and used for this evaluation. Therefore, the nonoptimized pseudo random interleavers used here are considered as interleavers with average performance. The optimization process of the optimized interleavers used in the current evaluation is described in [16] and based on the weight distribution of the overall turbo code and bit error probability simulations carried out for an AWGN channel. The particular turbo code interleaver with the most favorable performance at a bit error probability of 10^{-6} for each block size was chosen.

The simulation results will be discussed in the following. For an interleaver size of 600 bits at the target bit error probability of 10^{-6}, the turbo code using the optimized interleaver structure shows a gain of about 1 dB compared to the non-optimized turbo code. For the larger interleaver sizes of 1,200 bits and 4,800 bits, which were simulated equivalently to the size of 600 bits, the gain decreases. For the block size of 1,200 bits, the gain at the same target bit error probability is in the order of 0.5 dB, whereas no gain can be obtained in the case of an interleaver block size of 4,800 bits, as the simulations have shown. Therefore, interleaver

optimization is only necessary and feasible for small block sizes and, therefore, for low delay or low data rate services.

5.3.4 Constraint Length of Constituent Recursive-Systematic-Codes

In order to evaluate the performance improvement of turbo codes using constituent RSCs with constraint length 3 as compared to constraint length 4, an LCD service with 300 ms delay and a data rate of 144 kpbs was simulated for both constraint lengths. The indoor channel at a mobile speed of 3 km/h was chosen and frame by frame power control was applied. Antenna diversity was not taken into account. The simulated bit error probability, with five decoding iterations and constraint length 3, reaches a bit error rate of 10^{-6} at about 5 dB. The performance with constraint length 4 shows an improvement of about 0.1 dB for all bit error rates.

The computational complexity of the turbo decoder directly depends on the number of states of the trellis diagram of the constituent RSCs, whereas the number of states can be determined from the constraint length of the codes. The constraint lengths 3 and 4, which are related to a 4 and 8-state trellis diagram, respectively, are most interesting because implementation is feasible and performance is satisfying. As shown in Section 5.3.1, a turbo code using RSCs with constraint length 3 performs significantly better than other coding schemes with comparable complexity. Considering current simulation results, the performance of the 8-state turbo code is slightly better than the performance of the 4-state turbo code, with a gain about 0.1 dB for all bit error probabilities. This performance gain cannot be justified by complexity.

5.3.5 Concluding Remarks

The performance comparison presented in Section 5.3.1 showed that the turbo code outperforms the concatenated RS and convolutional code in almost all considered environments and parameter sets by 1 to 3 dB. Optimizing the code concatenation will reduce the gain of the turbo code by a small amount. For the presented services, a turbo code interleaver size of 2,400 bits is sufficient, if the interleaving is not optimized. Using optimized interleaving, the sufficient block size can be reduced to 600 bits. The complexity of the channel coding scheme is of major importance for the later implementation. In Section 5.3.4 it was shown that a turbo code using RSCs with constraint length 3 performs almost as well as one using RSCs with constraint length 4. In additional simulations the performance of a suboptimum turbo code implementation was evaluated, yielding the result that the performance does not significantly degrade and implementation is therefore feasible thanks to the reduced complexity. The presented results clearly show the superiority of the turbo codes in terms of performance and complexity compared to the concatenation of an RS code with a convolutional code. For more detailed results on the presented topics, please refer to [17].

5.4 OPTIMUM DISTANCE SPECTRUM CONVOLUTIONAL CODES

Since there is no known approach to find good convolutional encoders analytically, good convolutional encoders are normally found by performing a computer search. Such a search can be quite tedious since a large number of combinations must be tested. For a rate $R=1/n$ encoder with constraint length K, there are 2^{Kn} possible combinations. Due to this, previous work has often been restricted to finding maximum free distance (d_f) codes. The search must then go on until a code with maximum free distance is found (fulfilling the Heller bound) or until all combinations are tested. Since there usually are several codes with maximum free distance this approach is significantly less complex than an exhaustive search. The maximum free distance is an important parameter for Gaussian channels, but there are also other parameters that have impact on the error rate of convolutional codes. This has motivated a search for improved convolutional codes that have good performance on both AWGN and Rayleigh fading channels [18, 19].

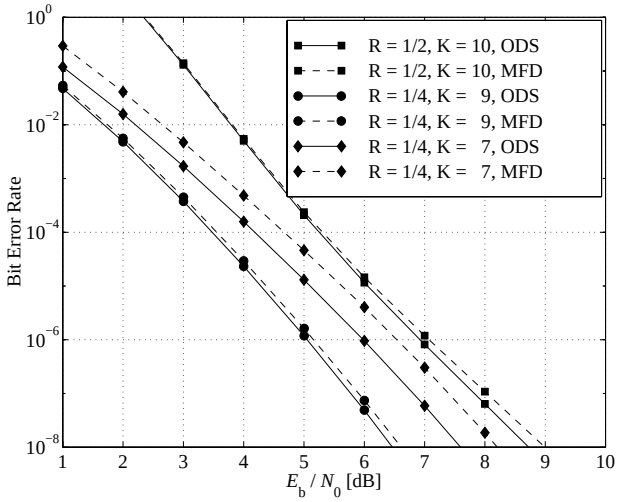

Figure 5.3 Upper bound on the bit error rate on an uncorrelated flat Rayleigh fading channel for ODS and maximum free distance (MFD) codes.

The codes described in this chapter are found using a criterion denoted the optimum distance spectrum (ODS) criterion. When performing a search using the ODS criterion, we compare the error weight coefficients of all possible encoders with maximum free distance d_f and select the one(s) with the smallest error weight coefficient value(s). If more than one encoder remains after this selection, we

continue comparing the coefficients for d_f+1, d_f+2, … until one encoder, or a set of equivalent encoders, remain(s). For more details on this search and the code tables, the reader is referred to [18, 19] and the reference therein. ODS codes are used as the basis for finding different types of good rate-compatible convolutional codes for CDMA systems in later sections. Figure 5.3 shows a comparison of the union upper bound on the bit error probability for maximum free distance codes found in [20] and [21], compared with ODS codes [18, 19] on a perfectly interleaved Rayleigh fading channel. We see that the improvement we get at no complexity cost is up to 0.6 dB.

5.5 CONVOLUTIONAL CODES FOR RATE MATCHING

Wireless communication systems are usually designed so that a channel has a fixed data rate. For example, in a TDMA system, a time slot has a fixed number of bits over a given time period and thus a fixed data rate. Similarily, a carrier frequency in a FDMA system, and a spreading code in a CDMA system with a fixed spreading factor correspond to a constant data rate, respectively. Multiple data rates can thus be achieved by allocating several of these fixed data rate channels, resulting in a multichannel system. A typical value of the data rate of a channel is in the order of 10 to 50 Kbps. However, the variability in, for example, speech is in steps in the order of a few Kbps, requiring a rate matching system as an interface to the allocated channels. In this section we propose using *rate-compatible convolutional* (RCC) codes for rate matching and error control in wireless multichannel systems. For further details, see [18, 22-24].

RCC codes are constructed such that lower code rates make use of the same code symbols as the higher code rate plus some extra redundancy symbols. This can easily be obtained by repeating symbols. However, repetition usually results in worse performance than nesting or puncturing. Thus, we have chosen to use *rate-compatible punctured convolutional codes* (RCPC) for the higher code rates and *nested convolutional codes* for the lower code rates.

RCPC codes [25] are constructed by puncturing a convolutional code of rate R=1/n and constraint length K, called the parent code. This code is completely specified by its generator polynomials. The puncturing is done according to a rate compatibility criterion, which requires that lower rate codes use the same coded bits as the higher rate codes plus one or more additional bit(s). The bits to be punctured are described by puncturing matrix consisting of zeros and ones, where zero means that the corresponding coded bit is punctured (deleted). The number of columns, or the puncturing period p, determines the number of code rates and the rate resolution that can be obtained. Generally, from a parent code of rate 1/n, we obtain a family of (n-1)p different codes with rates from 1/n up to p/(p+1). Due to the rate compatibility criterion, the code rate of RCPC codes can be changed during transmission and thus unequal error protection can be obtained [25, 26]. Another application for these codes is in hybrid type-II ARQ systems, as discussed in Section 5.8.2 and [27].

Nested convolutional codes [28, 29] are obtained by extending a code of rate 1/n to a rate 1/(n+1) code by searching for the best additional generator polynomial. It is obvious that this type of code family is rate-compatible, and the big advantage is the modular code design that reduces the complexity of the search for low-rate codes.

In [18, 23] we present RCPC codes with constraint lengths K=7-11 using rate R=1/4 ODS parent encoders. Furthermore, these code sets are extended using nested codes down to rate R=1/512. It is also interesting to note that the nested codes are maximum free distance codes. It is furthermore shown that a puncturing period of p=8 and parent code rate of R=1/4 is a good compromise between a flexible coding scheme with many rates and good performance. Given these parameters, the RCPC codes were shown to have a performance close to that of the unpunctured ODS codes at rates 1/2, 1/3, and 1/4. We can therefore conclude that the performance loss due to puncturing is very small.

As an example of rate matching, consider a DS-CDMA system where multiple data rates are obtained by a *multicode* scheme [9], letting each user use multiple spreading codes and transmit data on these in parallel. With fixed spreading there will be a number of fixed-rate channels available. If the system is to support any source rate, there is a need for matching the source rate to a multiple of the channel rate. By using the proposed RCC codes, we have many different code rates with different levels of error protection, and a flexible means of matching the source data rate to the rate of the parallel channels [22]. However, when lower rate coding is applied, more subchannels are needed to transmit the channel symbols. This results in more interference to the other users of the system. It is therefore of interest to investigate the performance of the multicode DS-CDMA system as the code rate is decreased. The efficiencies obtained for a bit error rate of 10^{-6} on a Gaussian and Rayleigh fading channel, respectively, are shown in Figure 5.4 for spreading factor N=128, and E_b/N_0=10 dB. As we see, the efficiency is increased with decreasing code rate. Thus, the extra coding gain obtained by reducing the code rate is larger than the reduction in the effective signal-to-noise ratio. We also see that the performance difference between Gaussian and Rayleigh fading channels decreases with decreased code rate. This is due to the increased diversity gain provided by the channel code as the code rate is reduced. With high diversity order, the performance on the Rayleigh fading channel approaches that of the Gaussian channel.

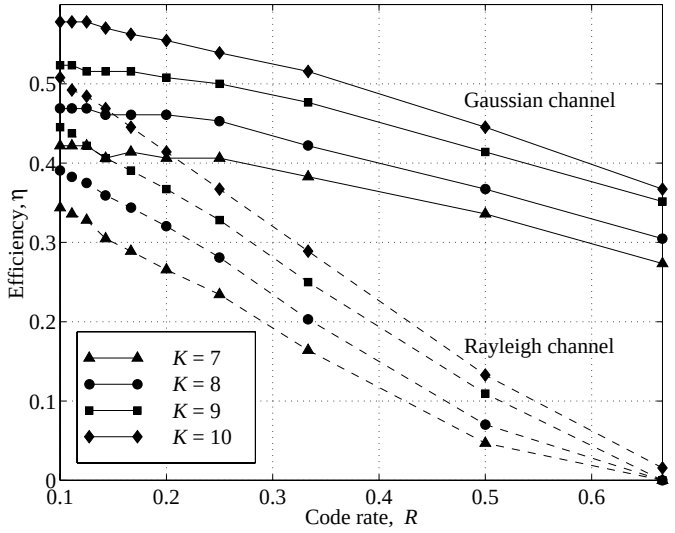

Figure 5.4 Achievable bandwidth efficiency for a multicode DS-CDMA system using rate-compatible codes on a Gaussian (solid lines) and Rayleigh fading channels (dashed line).

5.6 SEQUENTIAL DECODING OF CONVOLUTIONAL CODES ON FADING CHANNELS

Sequential decoding is a decoding technique for convolutional codes that received a lot of attention before the Viterbi algorithm was known. To obtain extremely low error probability with convolutional codes, very long constraint lengths must be applied. The Viterbi algorithm is then too computationally intensive. For such systems, sequential decoding is still an attractive decoding method, making decoding of constraint length 30 to 50 convolutional codes possible. Overviews of sequential decoding techniques can be found, for instance in, [2]. With sequential decoding, only a fraction of the code tree is actually searched, reducing the average computational load considerably. The great disadvantage is that the number of computations needed to decode a bit is a random variable with a Pareto distribution [2]. Therefore, we can never avoid input buffer overflows. However, the overflow rate is reduced by increasing the buffer size, or increasing the speed of the decoder. It is possible to evaluate for which E_b/N_0, corresponding to ρ=1 and ρ=2 respectively, the mean and variance of the number of computations are limited. Table 5.3 shows those values for a number of code rates using BPSK modulation on a Rayleigh fading channel. For more details on how these results are obtained, the interested reader is referred to the papers by Orten and Svensson [30, 31] where also other modulation methods and hard decision decoding are reported.

Table 5.3

Theoretical limits for sequential decoding of convolutional codes on Rayleigh fading channels for different code rates. Energy per information bit E_b/N_0 values are given in dB.

R	1/4	1/3	1/2	2/3	3/4	4/5	5/6	6/7	7/8	8/9
ρ=1	3.8	4.4	5.7	7.5	8.8	9.8	10.6	11.3	11.9	12.4
ρ=2	5.9	6.5	8.0	10.0	11.3	12.3	13.2	13.8	14.5	15.0

Figure 5.5 shows the overflow rate as a function of E_b/N_0 for hard and soft decisions on a Rayleigh fading channel using BPSK modulation obtained by simulations. We see that simulation results and theoretical limits match quite well. All theoretical results assume a memoryless channel that can be obtained only by perfect (infinite) interleaving. In Figure 5.6, we have therefore plotted the overflow rate for different interleaving depths. As we see from the figure, the loss is quite small if we can afford to use a 50×50 interleaver. Naturally, the loss increases as the interleaver size is reduced.

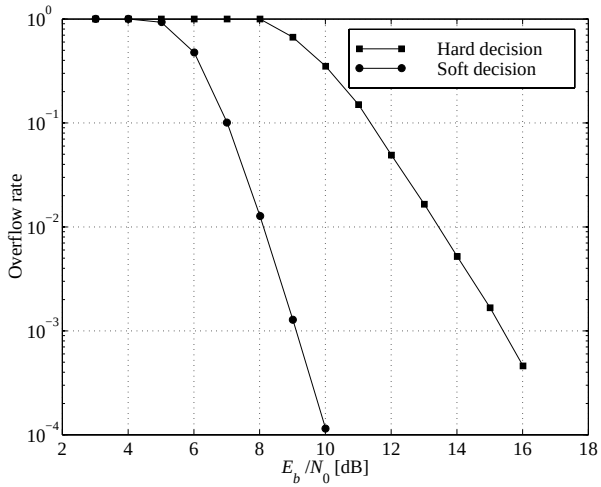

Figure 5.5 The overflow rate as a function of average E_b/N_0 for coherent BPSK with perfect interleaving, obtained by simulations. Results are shown for a hard decision and 8-level soft decisions. An overflow occurs when the total number of forward searches exceeds two times the data block length of 500 information bits.

For a Rayleigh fading channel, the calculation of the Fano metric used with sequential decoding is quite cumbersome. A natural way of avoiding this complexity is to quantize the signal and do a table lookup for each soft decision to find the metric. In [31] there is an evaluation on how the quantization should be done and the loss induced by quantization.

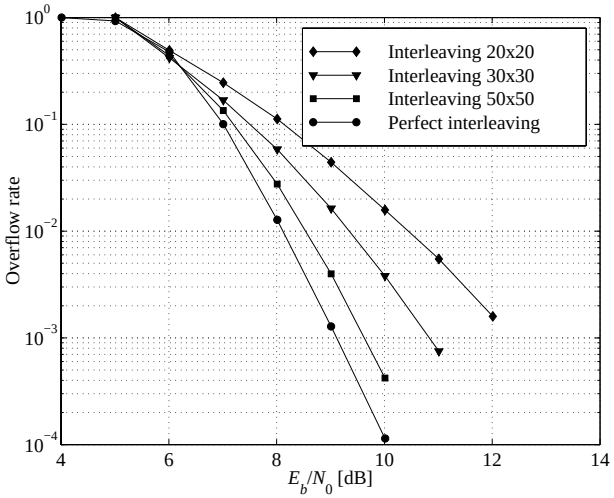

Figure 5.6 Overflow rate as function of E_b/N_0 for BPSK modulation with different interleaving depths and 8-level soft decisions, normalized Doppler frequency fdTs = 0.01.

5.7 CODE SPREAD CDMA

5.7.1 Low-Rate-Coded CDMA Based on Convolutional Codes

In DS-CDMA systems, the bandwidth is expanded by using spreading codes. Bandwidth expansion can also be obtained by the redundancy added by error correcting codes. In a conventional narrowband communication system, this bandwidth expansion is generally an undesired feature. However, for spread-spectrum systems, it has been shown that high efficiency is achievable by employing low-rate channel codes alone for bandwidth expansion [32, 33]. The conventional direct-sequence spreading operation may be viewed as repetition coding followed by randomization. It is of course possible to replace the repetition encoder by a designed channel encoder of the same rate. We will refer to spreading by channel codes only as *combined coding and spreading* or *code-spreading*. A limiting factor has been the lack of good low-rate codes. The work of [32] proposes the use of *orthogonal* convolutional codes [34], and in [35] these codes were modified into the class of *superorthogonal* convolutional codes.

Figure 5.7 shows a schematic of a code-spread CDMA system, where all bandwidth expansion is achieved by a low-rate (rate 1/*n*) convolutional code, producing *n*-coded symbols per information bit. These symbols are then interleaved, and randomized by a nonspreading, user-specific, long pseudo-random scrambling sequence. The *k*th user's signal, $s_k(t)$, is transmitted over the mobile radio channel, and at the receiver side, similar signals from other users (MAI) are added, producing the resulting received signal.

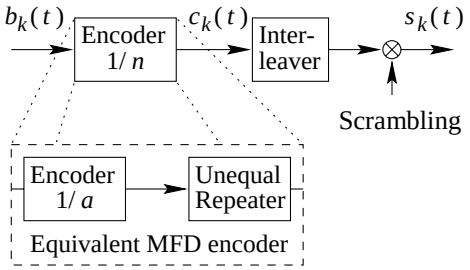

Figure 5.7 The code-spread CDMA system. The very low-rate MFD codes used for combined coding and spreading can be viewed as a higher rate 1/*a* code followed by a device repeating different encoded bits.

Frenger et al. presented low-rate convolutional codes for combined coding and spreading in [36, 37]. These codes are nested codes, obtained by starting with a rate $R = 1/4$ parent convolutional encoder. An advantage with these new codes is that they, in addition to having MFD, have an unequal repetition structure. Thus, the codes can be constructed as a rate 1/*a* code, where $a<<n$, followed by an unequal repeater. As an example, we show in Table 5.4 the generators of the low-rate code family with $K = 8$. We see that for a total spreading of 200, one generator is used 57 times, another 57 times, and other generators are used 28, 27, and 27 times, respectively. This structure greatly reduces the encoder and decoder complexities and may also used to facilitate synchronization.

Table 5.4

Example of encoders for rate $R = 1/n$ codes with constraint length $K = 8$, illustrating the unequal repetition structure of the code family. The table shows the generator polynomials in octal format (top row) and their frequencies.

n	231	247	273	275	327	337	345	353	373	375
4	1	0	1	0	1	0	0	0	0	1
17	1	3	1	3	3	0	3	2	1	1
18	1	3	1	3	3	1	3	2	1	1
100	1	28	1	14	25	12	13	4	1	1
200	1	57	1	28	53	27	27	4	1	1
500	1	143	1	71	139	69	70	4	1	1

In Figure 5.8, we show the calculated efficiency (the integer number of users that the system can support divided by the total spreading) on a Rayleigh fading channel at BER = 10^{-6} and $E_b/N_0 = 10$ dB, assuming perfect interleaving. The low-rate nested code used for the code-spread system has constraint length $K = 10$. Also shown are the results obtained with symbol and chip-interleaved conventional systems with a rate $R = 1/4$ ODS encoder of the same constraint length, and direct-sequence spreading with a random spreading sequence to the same total bandwidth. The efficiency of code-spread systems employing orthogonal codes

and superorthogonal codes are also plotted. We assume random spreading sequences for the conventional systems, and that all systems have an outer scrambling sequence that is pseudorandom and much longer than the bit duration. We further assume BPSK modulation and that the users transmit asynchronously. We see that the code-spread system using the presented low-rate encoders and no conventional spreading outperforms all the other schemes. Due to the dependence between code rate and constraint length, the superorthogonal codes can compete only when the spreading is 256. The conventional symbol-interleaved DS-CDMA system with rate 1/4 coding achieves less than 70 % of the efficiency obtained by the proposed code-spread system. As expected, the orthogonal codes have even worse performance, and achieve at best the same efficiency as the conventional system at a spreading factor equal to 256. For more information see [36, 37].

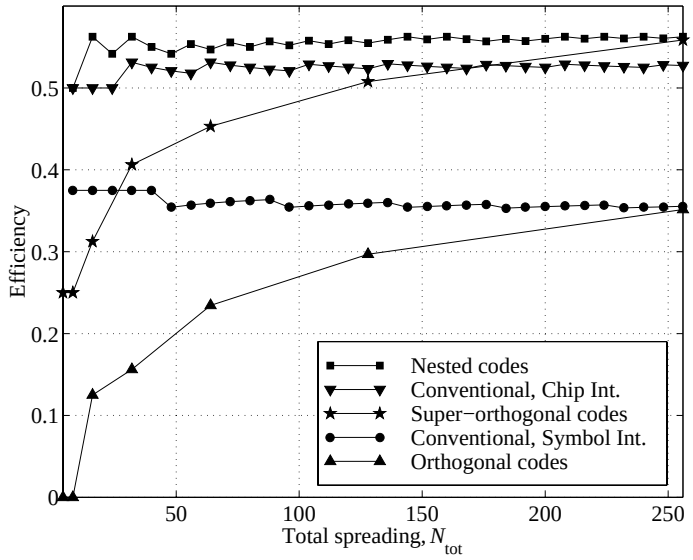

Figure 5.8 The efficiency of a code-spread system with constraint length $K = 10$ nested encoders for different spreading factors and bit error rate 10^{-6}. Also shown are the efficiency results of a conventional system using a $R = 1/4$, $K = 10$ convolutional code and code-spread systems using orthogonal and superorthogonal convolutional codes.

5.7.2 Interference Cancellation for Low-Rate Coded CDMA

The BER performance of a code-spread CDMA system employing PIC [38] is shown in Figure 5.9. The outputs of the channel decoders of each user are used to regenerate the signals to be canceled in the next IC stage. Results from simulations are shown using solid lines, and white and black markers are used for one stage and two stages of PIC, respectively. Using dashed lines, we also show analytical results obtained by approximating the interference from the other users as

Gaussian distributed and employing the union upper bound of the convolutional channel encoder. We define the load as the ratio between the total data rate of all users and the chip rate. We see that when reducing the number of users in the system, the BER decreases rapidly. Eventually a plateau is reached where the BER stays constant. At this plateau, effectively all interference is removed by the interference cancellation scheme, and thus we have reached the single user bound for the low-rate channel code used. We see that the performance of code-spread CDMA systems is greatly enhanced when combined with this kind of interference-reduction technique. Further details are given in [39].

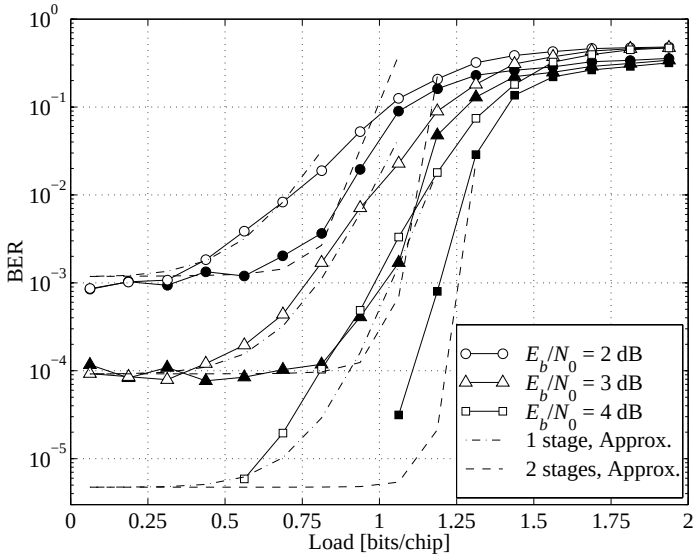

Figure 5.9 Bit error rate for the code-spread system with PIC versus the load for E_b/N_0 = 2, 3, and 4 dB. Simulated results for one stage (white markers) and two stages (black markers) of PIC, as well as analytical results (dash-dotted and dashed lines) are shown.

5.7.3 TCH Codes in CDMA

The new family of TCH (Tomlinson, Cercas, Hughes) codes [40, 41] was studied for the radio interface of a mobile receiver. TCH codes are a class of binary, nonlinear, nonsystematic, and cyclic block codes. The code word length is $n=2^m$, where m is any positive integer. The first polynomial in a TCH code, designated as *basic TCH polynomial* or B-TCH, is generated analytically and is then extended to increase the code set using known methods. It was shown in [41] that B-TCH polynomials can only be generated for specific values of the code length n, which are exactly the Fermat numbers minus one, i.e., 2, 4, 16, 256, and 65,536. A very important property of these polynomials is that its autocorrelation function is

always three-valued with values 0, –4, and n, regardless of the sequence length n, which makes its autocorrelation function nearly ideal for large n.

TCH codes were initially applied for error correction, either alone or concatenated with a Reed Solomon code. A tight upper bound for its probability of information bit error on an AWGN is available [41]. The performance has also been determined for other channel models, such as a Rayleigh fading channel [42]. The performance of TCH codes is similar to the performance of other error correction codes of the same length and rate, such as BCH codes .

The great advantage of TCH codes is therefore not in terms of coding gain but the simplicity and efficiency of its receiver. In fact, the structure of the receiver depicted in Figure 5.10 performs maximum likelihood soft-decision decoding in the frequency domain with a very small number of correlations. The TCH receiver shown needs only a cycle of one complex FFT, a complex multiplication, and a complex IFFT to perform 4n correlations.

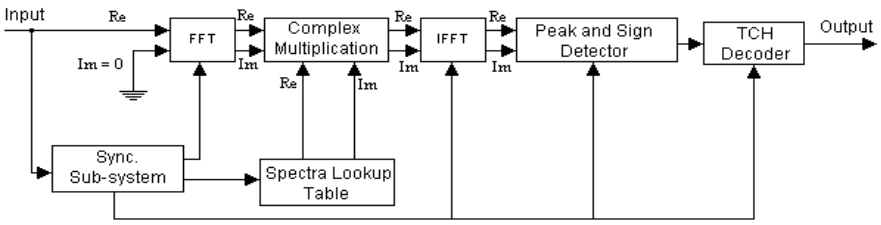

Figure 5.10 TCH receiver or TCH maximum likelihood decoder.

The TCH receiver shown needs only a cycle of one complex FFT, a complex multiplication, and a complex IFFT to perform 4n correlations. For instance, if we take a TCH(256, 15) code that has 32,768 code words, the TCH receiver needs only a maximum of 32 correlations in the frequency domain to identify the most likely code word sent, that is, a complexity gain in the order of 1,000.

The fact that TCH codes possess a good autocorrelation and, simultaneously, a well-behaved crosscorrelation function suggested its use in CDMA. In this case, the code words are taken as possible sequences. Moreover, it was found that several sets of sequences derived from B-TCH polynomials are orthogonal, although its use should be more appropriate for a synchronous CDMA system. A new approach was then considered for testing TCH codes in a normal asynchronous CDMA environment. Since TCH codes are inherently low-rate codes, which can be difficult to find in some applications [36], we took advantage of that fact and tested them in a so-called code spreading application, (i.e. with all the spreading done by the FEC code) (compare Section 5.7.1).

This situation was simulated for an asynchronous AWGN DS-CDMA channel, with an E_b/N_0 of 10 dB and an overall spreading factor of $N_{tot} = 32$. The results are shown in Figure 5.11, where we can observe that TCH codes allow a larger or equal system load than the other considered codes.

Similar results were obtained for an uncorrelated flat Rayleigh fading channel with perfect channel estimates [43]. Concluding, we say that TCH codes may be applied in both FEC and in a DS-CDMA system exhibiting a reasonable performance. Their major advantage relies on the structure of the TCH receiver, both in terms of simplicity of implementation and correlation speed, as desired for the mobile receivers of future generations.

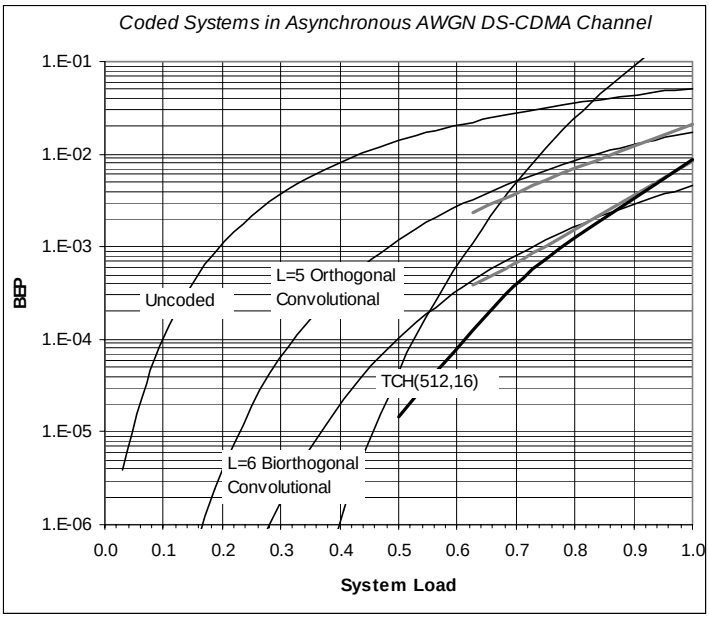

Figure 5.11 Upper bounds and simulation results on performance of various codes in an asynchronous AWGN DS-CDMA channel, E_b/N_0=10 dB, N_{tot}=32.

5.8 CODING FOR PACKET DATA TRANSMISSION

In some data applications, very low bit error probabilities are required. When a feedback channel is available, this may be obtained by using ARQ protocols. In these protocols, the transmitted data is encoded for error detection rather than error correction and detected errors at the receiver results in a generation of a retransmission request. This protocol is normally used with packet data switching, where a data packet of fixed length is transmitted independent of all other data over the channel. A good overview of this coding technique is given in [2].

The simplest form of ARQ, where the encoded information packet is retransmitted until it is received as a code word, is referred to as simple ARQ. By choosing an error detection code with a large minimum distance or free distance, the undetected error probability (the transmitted information is changed into another code word) can be made as small as required. The main drawback with

ARQ is that the throughput, defined as the inverse of the average number of coded bits needed to transmit one single information bit, becomes quite low unless the channel error probability is low.
Therefore, it is quite common to use error correction coding in combination with error detection coding in ARQ. These kinds of schemes are normally referred to as hybrid type-I ARQ schemes. Since some errors are corrected by the error correction code, the channel as seen by the error detection code improves and the number of retransmissions decrease. The main drawback is that the throughput is reduced by the code rate of the error correction code.

In general, the maximum throughput is given as the product of the code rates of the error correction code and the error detection code. In order to maximize throughput, this means that as little channel coding as possible should be used. This may be quite easy to obtain on static channels, where the channel coding can be optimized for the particular signal-to-noise ratio to be used. On time varying channels, like, for example, a mobile radio channel, the signal-to-noise ratio will instantaneously change such that some packets will be transmitted over a good channel, while others will be transmitted over a bad channel. Then there is no single coding scheme that optimizes the throughput, but an adaptive scheme is needed.

This can be obtained by using hybrid type-II ARQ schemes, which is a kind of code combining scheme. Code combining refers to a scheme, where for each information packet, previously received packets found to be in error are combined with the last received packet before decoding. This is equivalent to using an error correction repetition code and adjusting the code rate to the highest rate that gives no detected errors in the receiver. It is however, well known that repetition codes are inefficient for the given code rate, and therefore optimum error correction codes should be used in place of the repetition code. These optimum codes have to be designed such that they can be used with code combining and therefore need to be rate compatible. Below we consider such schemes based on both turbo codes (Section 5.8.1) and convolutional codes (Section 5.8.2). With convolutional codes, we also look at sequential decoding for long constraints lengths (Section 5.8.3), which makes the error detection code obsolete. In this scheme, the coding rate for error correction can be adapted to the channel and no error detection coding is needed. Therefore, this scheme has the prospect of optimizing the throughput.

5.8.1 Turbo Codes Applied to Type-II Hybrid ARQ Protocols

In order to evaluate the performance of turbo codes for packet data transmission with adaptive coding, two equivalent type-II hybrid ARQ schemes were defined, the first one using convolutional codes and the second one using turbo codes. These ARQ schemes will be described in Section 5.8.1.1. Identical link level simulations with TD-CDMA were carried out for both schemes, yielding comparable results. The obtained simulation results are described and discussed in Section 5.8.1.2, followed by some conclusions in Section 5.8.1.3.

5.8.1.1 Considered ARQ Schemes

A type-II hybrid ARQ protocol is considered using a CRC code for error detection and either a turbo code or a convolutional code for error correction. In both cases, the user information data block with a length of about 200 bits is first encoded for error detection. A CRC code with characteristics (232, 216) and the code polynomial $g_{ANSI}(x)=x^{16}+x^{15}+x^2+1$ generates 16- parity check bits appended to the original user data block, compare with [44]. In the case of the convolutional code, after CRC encoding, 8 tail bits are attached, which are used for trellis termination in the Viterbi decoder inside the receiver.

Then, the CRC encoded data block is encoded for error correction either by a convolutional encoder or a turbo encoder. The convolutional encoder has code rate $1/3$, constraint length 9, and generator polynomials (557, 663, 711) in octal. The turbo encoder has also code rate 1/3 and consists of two identical RSCs with generators (5, 7) in octal and constraint length 3. The outputs of the convolutional or turbo encoders are then multiplexed and mapped to three code words of the same length. The code words are transmitted using the selective repeat ARQ protocol. The number of buffer elements in the transmitter and receiver are assumed infinite. Additionally, the feedback channel is assumed to be error-free. Three different code rates 1, $1/2$, and $1/3$ can be achieved depending on the actual channel conditions.

It should be mentioned that all parameter settings and protocol-specific attributes were pragmatically chosen with the aim of not achieving an absolute performance measure but obtaining comparable results for the application of turbo codes and convolutional codes for ARQ protocols. For more detailed information on type-II hybrid ARQ protocols with rate-compatible, punctured convolutional codes, refer to [25, 27], and Section 5.8.2.

5.8.1.2 Simulation Results and Discussion

For the indoor and the pedestrian channels (as defined in Section 5.3.1) with a mobile speed of 3 km/h, the scheme using turbo codes needs an E_b/N_0 of 8.1 dB to obtain 144 Kbps, whereas the scheme using the convolutional code requires 8.6 dB. For the vehicular channel at 120 km/h, an E_b/N_0 of 10.0 dB and 10.5 dB is needed in the case of the turbo code and the convolutional code, respectively. These results are with a single receiver antenna. By introducing antenna diversity with two omnidirectional receiver antennas, a diversity gain of about 4 dB can be achieved, but the 2 dB loss for the vehicular channel still remains. The general conclusion based on the obtained results is that the gain of the turbo code is 0.5 dB. The comparison is justified by the fact that the computational effort of the two considered schemes are almost equal when five iterations are used with the turbo code as discussed in Section 5.3.1.

The performance of turbo codes strongly depends on the choice of the turbo interleaver and the block size. It was shown that the performance of turbo codes in the case of circuit switched services and in terms of the measured bit error

probability can be significantly improved by using optimized interleavers, especially in the case of very short block sizes around and below 600 bits [17]. In the current performance comparison, optimized interleavers were not utilized. Therefore, we assume that the performance of the turbo code using type-II hybrid ARQ protocol can be significantly improved if optimized turbo interleavers are applied. The use of longer data packets should also lead to a performance improvement in the case of the turbo code. Throughout the current evaluation, an ordinary turbo decoder was used, but the iterative turbo decoding process also has the potential of further performance improvement [45, 46].

5.8.1.3 Conclusions

The superiority of turbo codes over comparable coding schemes like concatenated Reed-Solomon and convolutional codes was already shown for the case of circuit switched services for various data rates and environments [17]. The current evaluation has proven that turbo codes are also well suited for the protection of packet data in the case of type-II hybrid ARQ protocols. It was shown that with turbo codes, a slightly higher throughput can be achieved than with convolutional codes, and it was stated that the performance of turbo codes can improve significantly. Although turbo codes are more beneficial in the case of larger block lengths, they are also superior in the case of packet data with relatively short blocks.

5.8.2 Convolutional Coding With ARQ

We present a comparison between four different hybrid type-II ARQ schemes, which are all based on RCPC codes. We will refer to them as schemes 2-5 [27]. The schemes are shown graphically in Figure 5.12.

Scheme 1 is a simple ARQ scheme with code combining and is used as reference. Data bits plus parity bits for error detection, form a packet of length L_C. Schemes 2-5 are hybrid type-II ARQ schemes that use RCPC codes. Scheme 2 was proposed in [47] and is used here as a comparison. The parent code rate is 1/3, the generator polynomials are (133, 165, 171) in octal form, the constraint length is 7 and a puncturing period of 2 is employed. Information bits, encoder tail bits, and CRC bits form a packet of length L_C or $2L_C$, respectively. This packet is encoded in the rate 1/3 parent code, resulting in a coded sequence of length $3L_C$ or $6L_C$, respectively. The coded sequence is now punctured such that the highest code rate is obtained (half of the bits are punctured for schemes 2-3 and one third of the bits are punctured for schemes 4-5). The nonpunctured bits are interleaved and transmitted over the channel. To transmit the coded bits, three channel blocks are used for scheme 3, two channel blocks are used for scheme 5, while for the other schemes only one channel block is used. The fading is assumed independent between channel blocks, but correlated within the block. The received samples are decoded in a Viterbi decoder and we assume that perfect channel state information (CSI) is available to the decoder. When the code rate is 1, the only available

redundant information is the encoder tail. If the CRC fails, a retransmission is requested, otherwise the packet is assumed to be received correctly.

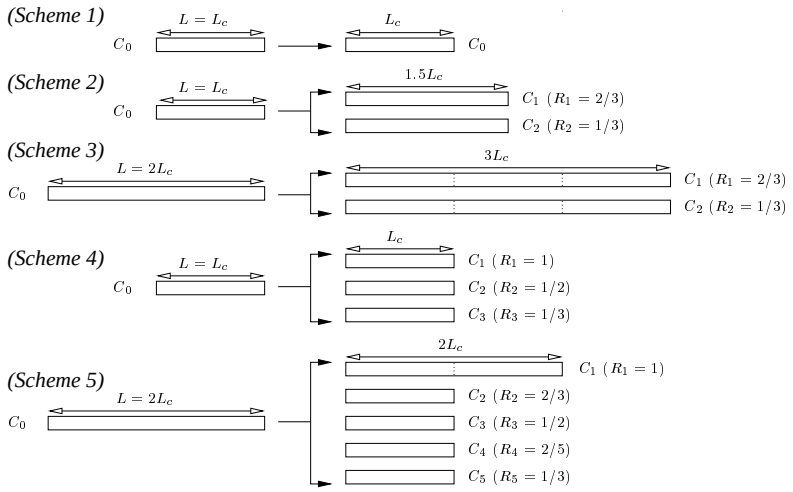

Figure 5.12 Schematic of the considered schemes.

When a retransmission is requested, the second highest code rate is used in the second decoding attempt. The code sequence is punctured according to the second highest code rate, but only those coded bits in the remaining code sequence that were punctured at the highest code rate are interleaved and transmitted. Now only one channel block is used to transmit the coded bits, except for scheme 3 where three blocks are used. In the receiver, these new bits are combined with the previously received bits and decoded in the Viterbi decoder. If the CRC fails, a retransmission is requested and the schemes repeat in a similar way (as shown in Figure 5.12). When all the rate 1/3 coded bits have been transmitted, the procedure is repeated over again. In the receiver, the new received bits are combined with all previously received bits before the Viterbi decoding is done.

In Figure 5.13, the throughput performance of schemes 1-5 on a Rayleigh fading channel with normalized (with the period of the coded symbol) Doppler frequency 0.001 are shown. The number of CRC bits is 16 in all cases and L_C=64. We see that scheme 5 performs better than all the other schemes for all SNRs. By starting at code rate 1, it maximizes the throughput at high SNRs when no error correcting coding is needed, which is not the case with schemes 2-3. At smaller SNRs, it tries to maximize the throughput by adapting the code rate to the SNR and only the increment between the code rates restricts this maximization. Moreover, the transmission delay of these new schemes is comparable to the delay of simple ARQ.

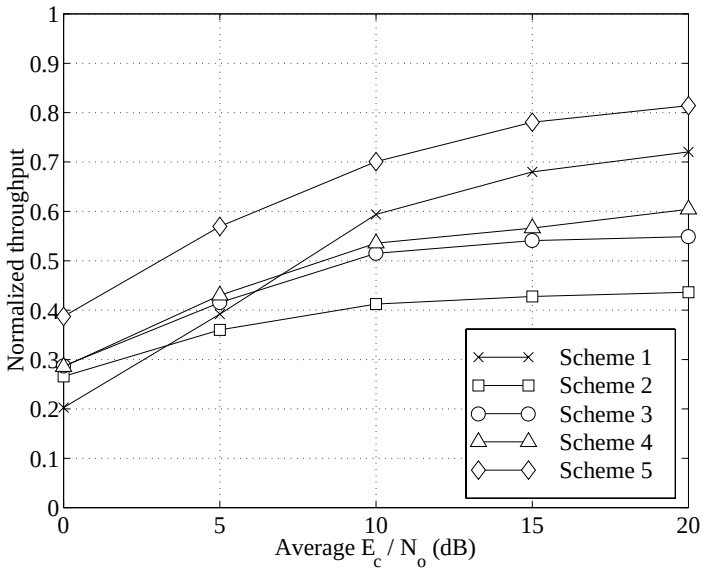

Figure 5.13 Simulated throughput for L_C=64 and normalized Doppler frequency 0.001.

These types of schemes have been thoroughly examined in [27, 48, 49]. Both the throughput dependency on Doppler frequency, packet length, and constraint length have been evaluated. It was found that a packet length on the order of 150 to 200 bits in most cases gives the best throughput. Furthermore, the constraint length of the code should not necessarily be chosen as large as possible, since the loss due to the extra tail bits in many cases is larger than the gain in throughput due to the increased error correction capability of the code. Scheme 5 was shown to be superior among the chosen schemes also for larger Doppler frequencies, and the throughput gain compared to simple ARQ, for example, becomes larger, since slow fading is advantageous for simple ARQ. Tailbiting Viterbi decoders [50] that do not require tail bits to be transmitted were also tested, but in almost all cases the throughput was reduced due to the increased bit error probability of these decoders. Optimum RCRC codes [51] in combination with RCPC codes were also evaluated but proved to have inferior throughput.

5.8.3 Hybrid ARQ Based on Sequential Decoding of Long Constraint-Length, Tailbiting Convolutional Codes

The conventional ARQ schemes described above require CRC bits in order to determine whether the packet contained errors or not. These check bits carry no information and they therefore reduce the system throughput. By using sequential decoding of long constraint length convolutional codes, the CRC bits are not needed. This is because the computational load, or decoding time, depends on the

channel quality. Decoding time can thus be used to indicate erroneous packets (timeout condition), see [52, 53] and the references therein.

Due to the long constraint lengths applied with sequential decoding, a large number of tailbits must be applied in conventional schemes to terminate the data packets and make them independent of each other. Since the number of tailbits is large, the reduction in throughput caused by the many tailbits is significant. By using long constraint length *tailbiting* convolutional codes and sequential decoding, it should therefore be possible to eliminate the loss caused by both CRC bits and tailbits. *Tailbiting* convolutional codes are obtained when using the last K–1 information bits in the data packet as the initial state of the convolutional encoder. The encoder is then forced into its initial state as it encodes the last part of the data packet. Thus, flush bits are not needed, and the throughput is significantly increased for long constraint length codes. The disadvantage with tailbiting codes is that the initial state must be estimated by the decoder. In the initial state estimation algorithm proposed by Orten in [52] and [53], a systematic encoder is applied, and $K–1$ systematic bits are used as an estimate on the initial state. If decoding can get started and proceed into the code tree, the initial state is assumed to be correct. Otherwise, a new estimate is obtained by shifting one bit position in the input data stream, and a new decoding attempt is made.

Figure 5.14 shows the throughput as a function of the packet length, with signal to noise ratio E_c/N_0=5dB, which gives a Pareto exponent ρ=2. As we see, analytical and simulated results match rather well. Tailbiting gives higher throughput than using a known tail for packet lengths above 300. The rapid degradation for packet lengths below 300 is due to initial state estimation failure. The algorithm requires that there must be $K–1$ consecutive error-free channel symbols in order to start decoding. By reducing the constraint length slightly, the probability of correct initial state estimation increases considerably, but this will increase the undetected error rate. However, the loss for the shorter packets is only critical for the lower SNRs. By increasing the E_c/N_0 to that required for rate 2/3 and 3/4, the initial state estimation has a low failure rate also for the shorter packets. For plots of the throughput in this case, see [52, 53].

Figure 5.15 shows the throughput as function of E_c/N_0 using an incremental redundancy ARQ scheme. Here we used packet length L_p = 200, L_p = 300, and L_p = 500 and a constraint length K=36 code. The results are obtained analytically. As we see, the gain in throughput by using tailbiting is increasingly significant as the packet length is reduced. However, for the lower signal-to-noise ratios the tailbiting scheme experiences some loss due to initial state estimation failure. For packet length L_p=200 and E_c/N_0 < 6 dB, the tailbiting scheme gives lower throughput than the conventional scheme with known tail. However in most cases, though, it will be more interesting to operate at a signal-to-noise-ratio yielding a higher throughput. Figure 5.15 shows that for a throughput equal to η=0.75 and packet length L_p=200, the gain achieved with tailbiting is close to 5 dB. More details can be found in [52] and [53].

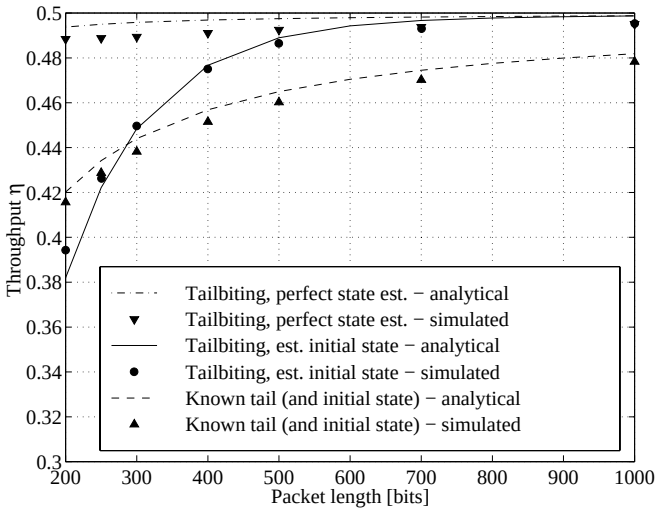

Figure 5.14 Throughput as function of the packet length in information bits. Signal-to-noise ratio is E_c/N_0=5dB, giving channel bit error rate approximately 0.064, and the convolutional encoder used for simulations is a constraint length K=36 systematic encoder with generator 714461625313 (octal notation).

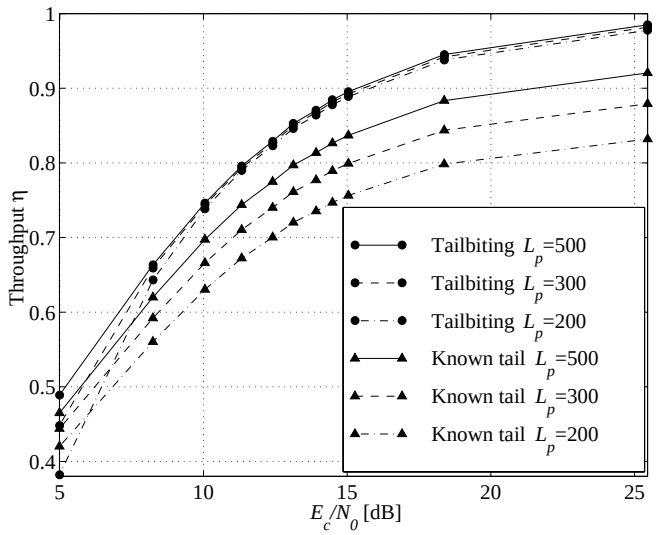

Figure 5.15 Analytical evaluation of the throughput as a function of the signal-to-noise ratio. Results are shown for packet lengths equal to L_p = 200, L_p = 300, and L_p = 500, and constraint length K=36, with and without known initial state (tail) and uncorrelated fading assuming an incremental redundancy ARQ scheme.

References

[1] J. G. Proakis, *Digital Communications*, McGraw-Hill: New York, 1995.

[2] S. Wicker, *Error Control Systems for Digital Communications and Storage*, Englewood Cliffs, New Jersey, Prentice Hall, 1995.

[3] C. Heegard and S. B. Wicker, *Turbo coding*, Kluwer Academic Publishers, Norwell, 1998.

[4] T. Ojanperä and R. Prasad, *Wideband CDMA for Third Generation Mobile Communications*, Norwell MA: Artech House, 1998.

[5] J. B. Anderson, T. Aulin, and C.-E. Sundberg, *Digital Phase Modulation*, Plenum Press, 1986.

[6] P. A. Laurent, "Exact and Approximate Construction of Digital Phase Modulations by Superimposition of Amplitude Modulate Pulses (AMP) ," *IEEE Transactions on Communication*, Vol. COM-34, No. 2, Feb. 1986, pp.150-160.

[7] M. Moretti, G.J.M. Janssen, and R. Prasad, "Binary and Multilevel Linearised GMSK: Spectrum Efficient Modulation Schemes for Personal Communications," *Proceedings FRAMES Workshop*, Göteborg, Sweden, 1998, pp. 47-52.

[8] M. Honkanen and S.G. Haggman, "New Aspects on Nonlinear Power Amplifier Modeling in Radio Communication System Simulations," *Proceedings IEEE Personal, Indoor and Mobile Radio Communications Conference*, Helsinki, Finland, 1997, pp. 844-848.

[9] T. Ottosson and A. Svensson, "On Schemes for Multirate Support in DS-CDMA Systems," *Wireless Personal Communications*, Kluwer Academic Publishers, Vol. 6, No. 3, March 1998, pp. 265-287.

[10] T. Ottosson, "Precoding in Multicode DS-CDMA Systems," *Proceedings IEEE International Symposium on Information Theory*, Ulm, Germany, 1997, p. 351.

[11] T. Ottosson, "Precoding for Minimization of Envelope Variations in Multicode DS-CDMA Systems," *Wireless Personal Communications*, Kluwer Academic Publishers, in press.

[12] C. Berrou, A. Glavieux, and P. Thitimajshima, "Near Shannon Limit Error-Correcting Coding and Decoding: Turbo Codes (1)," *Proceedings of IEEE International Conference on Communications*, Geneva, Switzerland, 1993, pp. 1064-1070.

[13] C. Berrou and A. Glavieux, "Turbo Codes: General Principles and Applications," *Proceedings of the 6th International Workshop on Digital Communications*, Tirrenia, Italy, 1993, pp. 215-226.

[14] ETSI Technical Report, "Universal Mobile Telecommunications System (UMTS); Selection Procedures for the Choice of Radio Transmission Technologies of the UMTS," TR 101 112, v. 3.2.0, April 1998.

[15] H. Koorapaty, Y. P. E. Wang, and K. Balachandran, "Performance of Turbo Codes with Short Frame Sizes," *Proceedings of IEEE Vehicular Technology Conference*, Phoenix, Arizona, May 1997, pp. 329-333.

[16] P. Jung, J. Plechinger, M. Doetsch and F. M. Berens, "A Pragmatic Approach to Rate Compatible Punctured Turbo Codes for Mobile Radio Applications," *Proceedings of the 6th International Conference on Advances in Communications and Control: Telecommunications/Signal Processing*, Grecotel Imperial, Corfu, Greece, 1997.

[17] T. Bing and F. Berens, "Parameter Evaluation for Turbo-Codes in the UTRA-TDD-Mode," *FRAMES Workshop*, Delft, The Netherlands, 1999, pp. 260-266.

[18] P. Frenger, P. Orten, T. Ottosson and A. Svensson, "Multirate Convolutional Codes," Tech. Rep. 21, ISSN-02083, Communication Systems Group, Department of Signals and Systems, Chalmers University of Technology, Sweden, April 1998.

[19] P. Frenger, P. Orten and T. Ottosson, "Comments and Additions to Recent Papers on New Convolutional Codes," submitted to *IEEE Transactions on Information Theory*, March 1999.

[20] K. J. Larsen, "Short Convolutional Codes with Maximal Free Distance for Rates 1/2, 1/3 and1/4," *IEEE Transactions on Information Theory*, Vol. IT-19, May 1973, pp. 371-372.

[21] J. P. Odenwalder, *Optimal Decoding of Convolutional Codes*, Ph.D. Dissertation, School of Engineering and Applied Sciences, University of California, Los Angeles, 1970.

[22] P. Frenger, P. Orten, T. Ottosson and A. Svensson, "Rate Matching in Multichannel Systems Using RCPC-Codes," *Proceedings IEEE Vehicular Technology Conference*, Phoenix, Arizona, 1997, pp. 354-357.

[23] P. Frenger, P. Orten, T. Ottosson, and A. Svensson, "Rate-Compatible Convolutional Codes for Multirate DS-CDMA Systems," *IEEE Transactions on Communications*, in press.

[24] P. Frenger, P. Orten, and T. Ottosson, "Convolutional Codes with Optimum Distance Spectrum," submitted to *IEEE Communications Letters*, July 1997.

[25] J. Hagenauer, "Rate-Compatible Punctured Convolutional Codes (RCPC Codes) and Their Applications," *IEEE Transactions on Communications*, Vol. 36, No. 4, May 1973, pp. 389-400.

[26] J. Hagenauer, N. Seshadri, and C.-E. Sundberg, "The Performance of Rate-Compatible Punctured Convolutional Codes for Digital Mobile Radio,"' *IEEE Transactions on Communications*, Vol. 38, No. 7, July 1990, pp. 966-980.

[27] S. Falahati and A. Svensson, "Hybrid Type-II ARQ Schemes for Rayleigh Fading Channels," *Proceedings International Conference on Telecommunications*, Vol. I, Chalkidiki, Greece, 1998, pp. 39-44.

[28] P. J. Lee, "New Short Constraint Length Rate 1/N Convolutional Codes Which Minimize the Required SNR for Given Desired Bit Error Rates," *IEEE Transactions on Communications*, Vol. COM-33, No. 2, February 1985, pp. 171-177.

[29] S. Lefrancois and D. Haccoun, "Search Procedures for Very Low Rate Quasi-Optimal Convolutional Codes," *Proceedings IEEE International Symposium on Information Theory*, Trondheim, Norway, 1994, p. 278.

[30] P. Orten and A. Svensson, "Sequential Decoding in Future Mobile Communications", *Proceedings IEEE International Symposium on Personal, Indoor and Mobile Radio Communications*, Helsinki, Finland, 1997, pp. 1186-1190.

[31] P. Orten and A. Svensson, "Sequential Decoding of Convolutional Codes for Rayleigh Fading Channels," *submitted to IEEE Transactions on Communications*, March 1999.

[32] A. J. Viterbi, "Very Low Rate Convolutional Codes for Maximum Theoretical Performance of Spread-Spectrum Multiple-Access Channels," *IEEE Journal on Selected Areas in Communications*, Vol. 8, No. 4, May 1990, pp. 641-649.

[33] J. Y. N. Hui, "Throughput Analysis for Code Division Multiple Accessing of the Spread Spectrum Channel," *IEEE Journal on Selected Areas in Communications*, Vol. SAC-2, No. 4, July 1984, pp. 482-886.

[34] A. J. Viterbi, "Orthogonal Tree Codes for Communication in the Presence of White Gaussian Noise," *IEEE Transactions on Communications*, Vol. COM-15, No. 2, April 1967, pp. 238-242.

[35] A. J. Viterbi, *CDMA Principles of Spread Spectrum Communication*, Reading, MA: Addison Wesley, 1995.

[36] P. Frenger, P. Orten and T. Ottosson, "Code-Spread CDMA Using Maximum Free Distance Low-Rate Convolutional Codes," submitted to *IEEE Transactions on Communications*, February 1998, revised February 1999.

[37] P. Frenger, P. Orten and T. Ottosson, "Code-Spread CDMA Using Low-Rate Convolutional Codes," *Proceedings IEEE International Symposium on Spread Spectrum Techniques and Applications*, Sun City, South Africa, 1998, pp. 374-378.

[38] S. Moshavi, "Multi-User Detection for DS-CDMA Communications," *IEEE Communications Magazine*, Vol. 34, No. 10, October 1996, pp. 124-136,

[39] P. Frenger, P. Orten and T. Ottosson, "Code-Spread CDMA with Interference Cancellation," accepted for publication in *IEEE Journal on Selected Areas in Communications*, 1999.

[40] F. Cercas, M. Tomlinson and A. Albuquerque, "TCH: A New Family of Cyclic Codes Length 2^m," *Proceedings IEEE International Symposium on Information Theory*, San Antonio, Texas, January 1993, p.198.

[41] F. A. B. Cercas, *A New Family of Codes for Simple Receiver Implementation*, Ph.D. Thesis, Technical University of Lisbon, Instituto Superior Técnico, Lisbon, March 1996.

[42] P. Sebastião, *Efficient Simulation of the Performance of TCH Codes Using Stochastic Models* (in Portuguese), M.Sc. Thesis, Instituto Superior Técnico, Lisbon, October 1998.

[43] L. Antunes, *The Application of TCH Codes in CDMA Systems for Mobile Communications* (in Portuguese), M.Sc. Thesis, Instituto Superior Técnico, Lisbon, 1999

[44] S. Lin and D. J. Costello Jr., *Error Control Coding: Fundamentals and Applications*, Englewood Cliffs, New Jersey: Prentice Hall, 1983.

[45] K. R. Narayanan and G. L. Stüber, "A Novel ARQ Technique Using the Turbo Coding Principle," *IEEE Communications Letters*, Vol. 1, No. 2, March 1997.

[46] K. R. Narayanan and G. L. Stüber, "Turbo Decoding for Packet Data Systems," *Proceedings. of the Communication Theory Mini Conference*, Phoenix, Arizona, 1997, pp. 44-48.

[47] H. Lou and A. S. Cheung, "Performance of punctured channel codes with ARQ for multimedia transmission in Rayleigh fading channels," *Proceedings of IEEE Vehicular Technology Conference*, Atlanta, Georgia, 1996, pp. 282-286.

[48] S. Falahati, T. Ottosson, A. Svensson, and L. Zihuai, "Hybrid Type-II ARQ Schemes Based on Convolutional Codes in Wireless Channels," *Proceedings FRAMES workshop*, Delft, The Netherlands, 1999, pp. 225-232.

[49] S. Falahati, T. Ottosson, A. Svensson, and L. Zihuai, "Convolutional Coding and Decoding in Hybrid Type-II ARQ Schemes on Wireless Channels," *Proceedings IEEE Vehicular Technology Conference*, Houston, Texas, 1999.

[50] R.V. Cox and C.-E. Sundberg, "An Efficient Adaptive Circular Viterbi Algorithm for Decoding Generalized Tailbiting Convolutional Codes," *IEEE Transactions on Vehicular Technology*, vol. 43, no. 1, February1994, pp. 57-68.

[51] L. Zihuai and A. Svensson, "New Rate Compatible Repetition Convolutional Codes," submitted to *IEEE Transactions on Information Theory*, February 1999.

[52] P. Orten, "Sequential Decoding of Tailbiting Convolutional Codes for Hybrid ARQ on Rayleigh Fading Channels," submitted to *IEEE Journal on Selected Areas in Communications*, March, 1999.

[53] P. Orten, "Sequential Decoding of Tailbiting Convolutional Codes for Hybrid ARQ on Wireless Channels," *Proceedings IEEE Vehicular Technology Conference*, Houston, Texas, 1999.